WIRELESS COMMUNICATIONS AND MOBILE COMPUTING
Wirel. Commun. Mob. Comput. (2015)
Published online in Wiley Online Library (wileyonlinelibrary.com). DOI: 10.1002/wcm.2651

RESEARCH ARTICLE

Theoretical analysis on caching effects in urban vehicular ad hoc networks

Chaoyi Bian[1], Tong Zhao[1], Xiaoming Li[1], Xiaojiang Du[2] and Wei Yan[1]*

[1] School of Electronics Engineering and Computer Science, Peking University, Beijing, China
[2] Department of Computer and Information Sciences, Temple University, Philadelphia, PA 19122, U.S.A.

ABSTRACT

Most applications in urban vehicular ad hoc networks (VANETs) rely on information sharing, such as real-time traffic information queries, and advertisements. However, existing data dissemination techniques cannot guarantee satisfactory performance when amounts of information requests come from all around the network. Because these pieces of information are useful for multiple users located in various positions, it is beneficial to spread the cached copies around. Existing work proposed caching mechanisms and conducted simulations for validation, but there is a lack of theoretical analysis on the explicit caching effects. Because of the complex urban environment and high mobility of vehicles, quantifying the caching effects on the VANET performance is quite challenging. We present the cache coverage ratio as the metric to measure the caching effects, and theoretical analysis is given based on reasonable assumptions for urban VANETs, through which we find the affecting factors include vehicle density, transmission range, and ratio of caching vehicles. We deduce the quantitative relationship among them, which have similar forms as the cumulative density function of an exponential distribution. We also consider the impact of vehicle mobility to predict the future cache effect on surrounding roads of the caching area. We conduct intensive simulations, which verify that the theoretical analysis results match quite well with the simulated reality under different scenarios. Copyright © 2015 John Wiley & Sons, Ltd.

KEYWORDS
VANET; cache; analysis; simulation

***Correspondence**
Wei Yan, School of Electronics Engineering and Computer Science, Peking University, Beijing, China.
E-mail: w@pku.edu.cn

1. INTRODUCTION

Vehicular ad hoc networks (VANETs) are special wireless ad hoc networks in which communication nodes are moving vehicles. VANETs have great potentials in the applications of driving safety, intelligent transportation, points-of-interest queries, and so on. The key function of these applications is information exchange. For instance, applications of location-related information queries deal with requests such as "Is there a traffic congestion on XXX Road?," "Are there available parking slots near XXX Restaurant?," and "What are the movies showing at XXX Cinema?," which contain the delivery of requests to the corresponding area and responses back. As another example, applications of location-based advertisements aim to deliver the information of promotions and sales to interested users, which include the subscription message delivery from users to the advertisement location and the information dissemination to the subscribed users.

However, existing routing and data dissemination mechanisms in VANETs cannot support these applications well especially when there are amounts of requests for the same information from various positions. Specifically, because of the complex urban VANET environment, packet delivery between distant vehicles is significantly affected by dynamic network topology, intermittent connectivity, and features of wireless communication. Existing researches show that the packet delivery ratio presents obvious drops, and the latency experiences significant increase when communication vehicles are distant [1,2].

Therefore, a direct way to improve the performance is to make multiple information copies cached at different positions. In other words, caching is exactly the technique that is beneficial for information sharing by distributing the desired information or data around (certain areas of) the network so that requests from anywhere can be quickly responded by nearby copies. Compared with deploying particular roadside infrastructure, choosing vehicles as cache carriers has the advantages of low cost and simple configuration. Besides, the routing and data dissemination mechanisms are scarcely affected.

Some empirical caching mechanisms are proposed for information-query applications. The simulation results prove that caching can bring nearly 100% improvement of the query success ratio in certain scenarios. And different caching mechanisms bring different benefits, up to 50% difference in the query delay [3,4]. On the other side, caching can introduce some extra overhead on storage and communication for cache management, which leads to a trade-off between overhead and benefits. Besides, there are also some other potential ways to apply caching in VANETs. For instance, the information centric networking architecture such as Named Data Networking [5] has built-in caching. When the architecture applies to VANETs, it is hopeful that some existing designs of caching mechanisms [6] can be helpful.

It is necessary to have a clear insight on the caching effects, that is, how much caching influences the VANET performance, which not only helps design and assess the caching mechanisms but also gives a guideline to deal with the overhead trade-off. However, the assessment of caching effects in VANETs confronts with great challenges. Owing to the high mobility of vehicles, cached copies also move quickly along with the vehicle carriers, which brings difficulties to characterize the cache effects in a long term. To the best of our knowledge, there is a lack of related work on studying the caching effects in VANETs with theoretical analysis.

In this work, we try to characterize the caching effects theoretically. We put forward the cache coverage ratio to quantify the caching effect. In brief, the cache coverage ratio is the ratio of vehicles that can access the data within certain hops, while the formal definition will be given later in Section 2. The main contents of our work include the following.

(1) We present the cache coverage ratio to measure the caching effects in the caching area. Then we give theoretical analysis based on reasonable assumptions of urban VANETs.
(2) We find the quantitative relationship among the cache coverage ratio, vehicle density, transmission range, and caching rate (ratio of caching vehicles) at any instant, which has similar forms as the cumulative density function of an exponential distribution.
(3) We consider the vehicle mobility to predict the future cache coverage ratio on surrounding roads of the caching area when vehicles with cached data move onto them afterwards. We give the quantitative relationship among the future cache coverage ratio, vehicle density, vehicle speed, transmission range, caching rate, and the signal phase cycle of traffic lights.
(4) We verify the theoretical analysis using intensive simulations with urban vehicle traffic simulator Simulation of Urban MObility (SUMO) [7], which show that our analysis results match quite well with the simulated reality.

Based on the theoretical analysis, we can compute the cache coverage ratio in specific scenarios, which is helpful for the estimation of caching effects, and we can also find the necessary caching rate for desired caching effects, thus guide the design of caching mechanisms for VANETs. Besides, our analysis also gives a hand to the trade-off between the caching overhead and benefit.

The rest of this paper is organized as follows. Section 2 gives the formal description of the caching problem in urban VANETs. Section 3 shows the theoretical analysis, and Section 4 demonstrates the simulations. Related work is given in Section 5. Finally, Section 6 concludes the whole paper.

2. PROBLEM STATEMENT

In this section, we present the formal description of the caching problem in urban VANETs.

2.1. Network model and assumptions

As described previously, VANETs are special wireless ad hoc networks in which vehicles moving on roads with high speeds are communication nodes. Vehicles communicate with each other through wireless multi-hop transmissions. Same as classic network modeling, we apply graph modeling for VANETs, that is, the network is abstracted to a graph $G(V, E)$. V represents the node set, that is, the set of vehicles, and E represents the edge set. An edge exists between a pair of nodes if the corresponding vehicles can communicate directly. Because of the dynamic network topology, a VANET is hard to be represented by a single static graph. Instead, the network snapshot at any instant can be viewed as a graph; thus, the dynamic network can be represented by a series of graphs $G(V, E, t)$, where t denotes the time instant. Graphs at different time instants are correlated. In other words, following some vehicle mobility rules, a graph $G(V, E, t)$ with a later time instant t "generates" from a graph $G(V, E, t')$ with an earlier t'. Nevertheless, we can still consider each graph as an independent one to investigate some concerned problems such as connectivity and caching effects. Because transmissions always happen at a certain moment, we can first quantify the caching effects by individual static network snapshots. Then we take the vehicle mobility into consideration to further quantify the future caching effects on surrounding roads of the caching area.

To simplify the modeling, we make some abstractions and assumptions listed as follows.

(1) We abstract the urban road topology to a Manhattan-like grid, that is, all roads have the same length, and there are only horizontal and vertical roads.
(2) We assume that the vehicle headway (i.e., distance between vehicles) follows a certain distribution. Sorts of distributions are proposed and applied

in existing work, including exponential distribution [8], Gamma distribution, and log-normal distribution [9]. Our analysis can be performed with any certain distribution, but for simplicity, we use the exponential distribution in the following analysis. And we assume the vehicle density is constant so that the vehicle headway is exponentially distributed with the same rate parameter across roads. But the vehicle density near intersections is higher, which indicates a larger rate parameter for zones near intersections.

(3) We assume the transmission range of a vehicle is a round disk, and all vehicles have the same transmission radius. Vehicles can communicate directly if the distance between them is not greater than the transmission radius. And we assume the transmission radius is much larger than the road width so that we neglect the affects of road width.
(4) We assume simple traffic lights with fixed signal phase cycles are deployed at intersections, and vehicles have fixed turning probabilities.
(5) We assume that the vehicle speed is basically stable in non-intersection zones, which is close to the speed limit of roads.
(6) We assume that each vehicle in the caching area has the same probability to have a cached copy for a specific piece of data, so that caching nodes are uniformly distributed. This probability is equal to the expected caching rate.
(7) We do not consider the packet loss because of channel fading or interference in the model analysis.

Among the aforementioned abstractions and assumptions, the fourth and fifth assumptions are only useful in the analysis of mobility impacts, while the others are used in the general modeling.

2.2. Formulation and notations

Under the network model and assumptions described previously, we propose the cache coverage ratio as follows.

Definition 1. *A vehicle is called to be n-hop covered if there exists at least one path of n hops or less between the vehicle and any vehicle with cached data.*

In the aforementioned definition, the cached data denote the specific piece of data that we are concerned with.

Definition 2. *The n-hop cache coverage ratio of an area is defined as the ratio of vehicles that are n-hop covered, that is, the number of vehicles that are n-hop covered divided by the total number of vehicles.*

The n-hop cache coverage ratio measures the caching effects well, because a high ratio means that most vehicles can obtain the desired data with no more than n hops, and a low ratio means that amounts of vehicles have to exchange information through a long path. Thus, the cache coverage ratio has a direct relationship with the success ratio and latency of data access, that is, a high cache coverage ratio usually means a high success ratio and small latency, while a low cache coverage ratio often comes with a low success ratio and large latency.

Table I. Notations.

Notation	Description
L	Grid length of the road network.
R	Transmission radius of nodes.
r	Radius of intersection zones.
λ_1	Rate parameter for intersection zones.
λ_2	Rate parameter for non-intersection zones.
μ	Probability that a node is a caching node.
Φ_n	n-hop cache coverage ratio.
v	Node speed in non-intersection zones.
T	Signal phase length of cyclic traffic lights.

Then we present the formal problem description of caching effects. In a graph $G(V, E)$ abstracted from a VANET at some instant, nodes are positioned with exponentially distributed intervals on an L-length grid, and an edge exists between two nodes if their distance is not greater than R. The rate parameters for intersection and non-intersection zones are λ_1 and λ_2, respectively. Here, we define the intersection zones to be zones within the distance r of intersection points. Besides, each node in the caching area has the same probability μ to be a caching node. The first problem is to compute the n-hop cache coverage ratio Φ_n of the caching area. Then we consider the impacts of node mobility given the condition that the node speed in non-intersection zones remains stable around v, and the cyclic traffic lights at intersections have a fixed signal phase length of T (i.e., duration of red/green light). The second problem is to compute the future n-hop cache coverage ratio on the surrounding roads of the caching area. The related notations are listed in Table I for clarity.

3. THEORETICAL ANALYSIS

In this section, we present the theoretical analysis on the cache coverage ratio with details.

3.1. Snapshot analysis

We first investigate the VANET snapshots to study the cache coverage ratio at certain instants.

3.1.1. One-hop cache coverage ratio.

As a start, we quantify the one-hop cache coverage ratio, which can be approximately computed as follows.

$$\begin{aligned}\Phi_1 &= |V_C|/|V| \approx E(|V_C|)/E(|V|)\\ &= \frac{\sum_{RS} E\left(|V_C^{RS}|\right)}{\sum_{RS} E(|V^{RS}|)}\\ &= \frac{\sum_{RS} P_1^{RS} E(|V^{RS}|)}{\sum_{RS} E(|V^{RS}|)}\end{aligned} \tag{1}$$

V_C denotes the set of one-hop covered nodes, V^{RS} and V_C^{RS} denote the set of nodes and one-hop covered nodes on a specific road segment (RS), and P_1^{RS} denotes the probability that a node on the road segment is one-hop covered. Because $E(|V^{RS}|)$ can be easily computed based on the exponential distribution, the main concern becomes the computation of P_1^{RS}. A node is one-hop covered if it is a caching node or it is a neighbor of a caching node. Therefore, we have Equation (2), in which Q_1^{RS} denotes the probability that a node is a neighbor of a caching node on the road segment.

$$P_1^{RS} = \mu + (1-\mu)Q_1^{RS} \tag{2}$$

To compute Q_1^{RS}, we have the following theorem.

Theorem 1. *The probability that a node located at x on the corresponding road segment in Figure 1 has a neighbor caching node that can be computed as follows.*

$$Q_1^{RS1}(x) = 1 - e^{-\lambda_2 \cdot 2R \cdot \mu},$$

$$Q_1^{RS2}(x) = 1 - e^{[-\lambda_1(r+R-x)-\lambda_2(x+R-r)]\cdot\mu},$$

$$Q_1^{RS3}(x) = 1 - e^{\left[-\lambda_1(r+R-x)-\lambda_2(x+R-r)-\lambda_1\cdot 2\sqrt{R^2-x^2}\right]\cdot\mu},$$

$$Q_1^{RS4}(x) = 1 - e^{\left[-\lambda_1(3r+R-x)-\lambda_2\left(x+R+2\sqrt{R^2-x^2}-3r\right)\right]\cdot\mu},$$

$$Q_1^{RS5}(x) = 1 - e^{\left[-\lambda_1\cdot 4r-\lambda_2\left(2R+2\sqrt{R^2-x^2}-4r\right)\right]\cdot\mu}$$

Proof. See Appendix A. □

Combining the aforementioned equations, the one-hop cache coverage ratio can be computed. Note that for RS2∼RS5, Q_1^{RS} (also P_1^{RS}) depends on the exact node position, thus the expressions of $E(|V_C^{RS}|)$ in Equation (1) change to integral shown as follows.

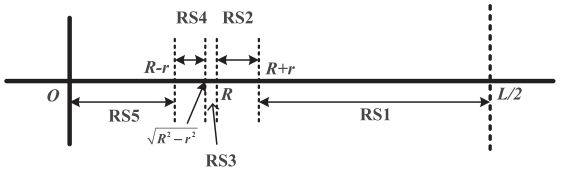

Figure 1. Dividing of road segments for computation of cache coverage ratio.

$$E\left(|V_C^{RS2}|\right) = \lambda_2 \int_R^{R+r} P_1^{RS2}(x)\mathrm{d}x,$$

$$E\left(|V_C^{RS3}|\right) = \lambda_2 \int_{\sqrt{R^2-r^2}}^{R} P_1^{RS3}(x)\mathrm{d}x,$$

$$E\left(|V_C^{RS4}|\right) = \lambda_2 \int_{R-r}^{\sqrt{R^2-r^2}} P_1^{RS4}(x)\mathrm{d}x,$$

$$E\left(|V_C^{RS5}|\right) = \lambda_2 \int_r^{R-r} P_1^{RS5}(x)\mathrm{d}x + \lambda_1 \int_0^r P_1^{RS5}(x)\mathrm{d}x$$

3.1.2. N-hop cache coverage ratio (N>1).

We continue to compute the n-hop cache coverage ratio. Similar to Equation (1), the ratio can be computed as follows.

$$\Phi_n \approx \frac{\sum_{RS} P_n^{RS} E\left(|V^{RS}|\right)}{\sum_{RS} E\left(|V^{RS}|\right)} \tag{3}$$

P_n^{RS} denotes the probability that a node on the road segment is n-hop covered. Also similar to Equation (2), we have Equation (4) in which Q_n^{RS} denotes the probability that a node locates in the n-hop range of a caching node on the road segment.

$$P_n^{RS} = \mu + (1-\mu)Q_n^{RS} \tag{4}$$

However, the determination of the accurate n-hop range is rather complex. Thus, we give an upper bound and an approximate computation method instead. The upper bound is based on the fact that the n-hop range with the transmission radius of R cannot be greater than the one-hop range with the transmission radius of nR. As shown in the succeeding text, Φ_n^R denotes the n-hop cache coverage ratio with the transmission radius of R, and Φ_1^{nR} denotes the one-hop cache coverage ratio with the transmission radius of nR.

$$\Phi_n^R \le \Phi_1^{nR} \tag{5}$$

The approximate method is based on the computation of expected one-hop distance, that is, the distance to the farthest node within the transmission range. We have the following theorem for the computation of expected one-hop distance.

Theorem 2. *If the transmission radius is R, and the node interval follows the exponential distribution with the rate parameter of λ, the expected one-hop distance E(D) on straight roads can be computed using Equation (6).*

$$E(D) = R - \frac{1-e^{-\lambda R}}{\lambda} \tag{6}$$

Proof. See Appendix B. □

Then the n-hop range can be approximated by $2[(n-1)E(D)+R]$. Thus, we can compute Q_n^{RS} as follows.

$$
\begin{aligned}
Q_n^{RS} &= 1 - P(\text{no caching node in the } n\text{-hop range}) \\
&\approx 1 - e^{-\lambda \cdot 2[(n-1)E(D)+R]\mu} \\
&= 1 - e^{-2\mu[\lambda nR-(n-1)(1-e^{-\lambda R})]}
\end{aligned} \tag{7}
$$

3.2. Analysis of mobility impacts

We make a step further to study the mobility impacts on the caching effects. The most significant impact of mobility is the movement of caching nodes, which affects the cache coverage ratio in surrounding areas. Therefore, we focus on intersections to study their impacts on incoming vehicle flows so as to predict the future cache coverage ratio on roads one (or more) intersection away from the caching area. Our analysis method is a sort of "framework," which can be extended to different kinds of intersections, and we show the ones with simple cyclic traffic lights as a typical example.

3.2.1. Intersection modeling.

The most important part of the analysis is the modeling of intersections. We use intersections with simple traffic lights deployed as the analytic focus. Specifically, we consider the following scenario and problem.

(a) A simple traffic light with fixed signal phase cycles is deployed at a typical intersection in a Manhattan-like grid road network. "Simple" means that there are no special lights for left/right turns, that is, left-turn vehicles share the same lights with the straight-going ones and right-turn vehicles can always pass. "Fixed" means that both the green and red lights always last for a certain duration.
(b) One or more vehicle flows come to the intersection from roads located in the caching area. Thus, these incoming vehicles have a certain caching rate. Besides, the vehicles have fixed turning probabilities at the intersection. The problem is "what is the future cache coverage ratio on the roads that the outgoing vehicle flows will move onto after passing through the intersection?"

We observe that the outgoing vehicle flow presents a periodic two-phase change according to the changes of traffic lights. As shown in Figure 2, in the first phase (left figure), the north-direction outgoing flow consists of the straight-going flow from south and right-turn flow from east, while in the second phase (right figure), the outgoing flow is made up of the right-turn flow from east and the left-turn flow from west.

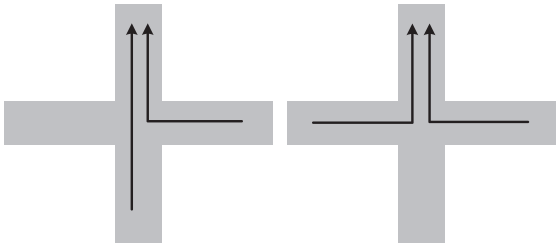

Figure 2. Periodic two-phase change of vehicle flows.

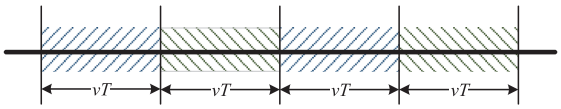

Figure 3. Periodic changes of vehicle distribution on the outgoing road.

Under the assumption that vehicles move with a stable speed, the distance between outgoing vehicles of an incoming flow after passing an intersection follows the exponential distribution with a rate parameter equal to that of the incoming flow multiplied by the turning probability. Besides, incoming flows from different directions are independent, so the distance between outgoing vehicles follows the exponential distribution with a rate parameter equal to the sum of each rate parameter multiplied by the corresponding turning probability.

Taking the north road in Figure 2 as an instance, the outgoing vehicles present a periodic change in the distribution as shown in Figure 3. The length of each segment is vT, in which v denotes the vehicle speed in non-intersection zones, and T denotes the signal phase length of cyclic traffic lights, that is, the duration of a signal light in a cycle.

3.2.2. One-intersection-away roads.

Based on the previous analysis, we can easily obtain the cache coverage ratio on roads one-intersection away from the caching area. The deduction process is quite similar as that in Section 3.1. Because of the complexity of formulas, we only show the basic ideas with a simple result in detail as the typical example.

Formula 1 (Simple Computation Method)**.** *In the one-intersection scenario shown in Figure 2, when only the vehicles coming from south have a certain caching rate, we can use Equation (8) to compute the approximate future one-hop cache coverage ratio on the north road.*

$$
\begin{aligned}
\Phi_1 \approx \frac{1}{4\mu p_s \lambda vT} \{ & \mu p_s(1 + 4\lambda R + 2\lambda vT) - 2 \\
& + e^{-4\mu p_s \lambda R}(2 - \mu p_s) \cdot \\
& [1 + \mu p_s(2R - vT)\lambda] \}
\end{aligned} \tag{8}
$$

Deduction. The deduction process of Equation (8) is similar as that in Section 3.1. So we only show the main steps as follows.

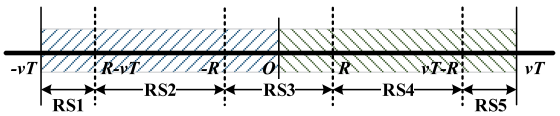

Figure 4. Dividing of road segments for computation of cache coverage ratio.

First, we have the following equations similar to Equation (1).

$$\begin{aligned}\Phi_1 &= |V_C|/|V| \approx E(|V_C|)/E(|V|)\\ &= \frac{\sum_{RS} E\left(|V_C^{RS}|\right)}{\sum_{RS} E(|V^{RS}|)}\\ &= \frac{\sum_{RS} 2\lambda \int_{RS} P_1^{RS}(x)\mathrm{d}x}{2\lambda \cdot 2vT}\end{aligned}$$

The last step can be explained as follows. The vehicle headway in the one-direction incoming flow follows the exponential distribution with the rate parameter of λ, so we use 2λ for two directions. And our computation focus is a $2vT$-long road segment consisted of a two-phase cycle as shown in Figure 4.

Then we can apply the similar method to compute $P_1^{RS}(x)$ as that in Equation (2) and Theorem 1 based on the dividing of road segments in Figure 4. We let the first half $[-vT, 0)$ corresponds to the left phase in Figure 2, and the second half $[0, vT)$ to the right one. Thus, we have the following formulas, in which p_s denotes the straight-going probability of vehicles at the intersection.

$$\begin{aligned}P_1^{RS1}(x) &\approx 1 - \left(1 - \frac{1}{2}p_s\mu\right) e^{-2\lambda(x+R+vT)\mu\cdot p_s},\\ P_1^{RS2}(x) &\approx 1 - \left(1 - \frac{1}{2}p_s\mu\right) e^{-2\lambda\cdot 2R\mu\cdot p_s},\\ P_1^{RS3}(x) &\approx 1 - \left(1 - \frac{1}{2}p_s\mu\right) e^{-2\lambda(R-x)\mu\cdot p_s},\\ P_1^{RS4}(x) &= 0,\\ P_1^{RS5}(x) &\approx 1 - \left(1 - \frac{1}{2}p_s\mu\right) e^{-2\lambda(x+R-vT)\mu\cdot p_s}\end{aligned}$$

Two approximations are included. The first one is the ratio of cached vehicles on the outgoing road, which we use $\frac{1}{2}p_s\mu$ as the approximate value. The second one is the passing through of waiting vehicles at intersections when traffic lights turn green. We directly multiply the rate parameter by two, which reflects the total vehicle number in the phase but cannot represent the distribution.

Combining the aforementioned equations, Equation (8) can be obtained.

When the vehicles coming from east, south, and west all have a certain caching rate, a similar deduction process as mentioned previously can be applied to compute the approximate future cache coverage ratio of the north road. The only difference is the ratio of caching vehicles on the road segments, which also include the left-turn vehicles from east and right-turn vehicles from west besides the straight-going vehicles from south. We abbreviate the concrete formulas and the deductions that are similar as that mentioned previously.

A simplified part in the aforementioned computation is the modeling of the passing through process of vehicles waiting at the intersection when traffic lights turn green, which generates a uniform vehicle distribution on the outgoing road. Thus, we can refine the method by counting this uniform distribution into computation. We abbreviate the concrete formulas due to complexity.

For n-hop cache coverage ratio ($n > 1$), the same approximation method as that used in Section 3.1 can be applied; thus, we do not repeat here.

3.2.3. Farther-away roads.

As for the farther-away roads that are two or more intersections away from the caching area, the computation method is similar. Briefly speaking, whenever vehicle flows come to a new intersection, we can apply the intersection modeling described previously to characterize the outgoing flow, thus to compute the future cache coverage ratio on roads after the intersection.

Taking two-intersection-away roads as an example, when vehicles that pass through the first intersection come to the second one, we can apply the computation method for one-intersection scenario with different parameters. For instance, in the simple method for the one-flow scenario, $\frac{1}{2}p_s\mu$ is replaced by $\frac{1}{2}p_s^2\mu$ in the computation of P_1^{RS} on the north-outgoing road. This deduction process can be easily extended to farther-away roads, although with accumulated errors.

4. SIMULATION

We conduct intensive simulations to verify the theoretical analysis. We choose SUMO [7] (version 0.21) to generate the vehicle traffic, which is based on the realistic microscopic car-following model of vehicles. So the generated mobility trace represents the reality to a certain extent, thus more persuasive in the validation of our analysis. In the following, we will describe the simulation environment and results in detail.

4.1. Validation of analysis on snapshots

First, we present the simulation details for the validation of analysis on snapshots described in Section 3.1.

4.1.1. Simulation scenario.

We use a Manhattan-like grid road network with a grid length of 400 m, which contains 30 road segments in each row and also 30 road segments in each column. Thus, the total area is $12 \times 12\,\mathrm{km}^2$. The maximum vehicle speed is 40 km/h. Initially, vehicles are randomly located in the sce-

nario, and later, vehicles only enter or leave the scenario from boundaries. We set a long trip for each vehicle so that the total number of vehicles does not fluctuate greatly during the simulation. Note that in this simulation scenario, the vehicle headway is determined by the microscopic car-following model, which is more realistic compared with the exponential-distribution assumption. Besides, we do not count the vehicles positioned near the map boundaries in the following results.

4.1.2. Validation results.

We present the detailed results in five parts. First, we present the validation results in the scenarios with one lane in each direction and the default SUMO car-following model (Part a and b), and then we show the results that prove that the number of lanes (Part c) and the choice of different car-following models (Part d) do not have significant effects. Finally, we also change the street length setting (Part e) to check the validity of the analysis.

(a) *Rate parameters:* We need to obtain the rate parameters used in our theoretical analysis first. Because we assume the vehicle headway follows an exponential distribution, the mean of which equals to the reciprocal of the rate parameter, that is, $1/\lambda$. So the rate parameter λ can be obtained by counting the mean vehicle density in simulations.

We choose the snapshot at 300 s for analysis because the simulation scenario experiences a variation because of the initial uniform vehicle positioning that becomes steady at about 200 s. We find that there is an obvious difference between the vehicle density around intersections and that in non-intersection zones, and setting the radius of intersection zones to 15 m achieves the greatest difference, which is used in the following results.

Table II lists the average values of rate parameters in the simulation scenarios with different total vehicle numbers. λ_1 and λ_2 denote the rate parameter for intersection and non-intersection zones, respectively, while λ denotes the rate parameter for overall zones without the distinction for intersections.

Table II. Values of λ.

Vehicle number	λ_1	λ_2	λ
$\sim 5,000$	0.02398	0.005545	0.006880
$\sim 6,000$	0.02856	0.006624	0.008218
$\sim 7,000$	0.03288	0.007710	0.009540
$\sim 8,000$	0.03757	0.008773	0.01087
$\sim 9,000$	0.04234	0.009830	0.01219
$\sim 10,000$	0.04703	0.01093	0.01356
$\sim 11,000$	0.05141	0.01202	0.01488
$\sim 12,000$	0.05552	0.01313	0.01621
$\sim 13,000$	0.05946	0.01429	0.01758
$\sim 14,000$	0.06273	0.01548	0.01891
$\sim 15,000$	0.06590	0.01669	0.02027
$\sim 16,000$	0.06887	0.01795	0.02165

(b) *Cache coverage ratio:* Then we conduct simulations to verify the analysis on cache coverage ratio. All results presented in the succeeding text is an average of 50 simulation runs.

Figure 5 shows the plots for one-hop cache coverage ratios when the transmission radius is 150 m. The *x*-axis represents the caching probability, and the *y*-axis represents the cache coverage ratio. As is clearly observed, the results from theoretical analysis match very well with sim-

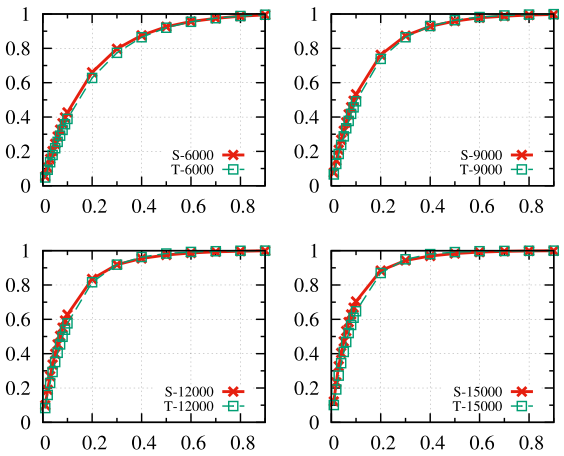

Figure 5. Comparison between simulations and theoretical analysis with the transmission radius set to 150 m. The *x*-axis and *y*-axis represent the caching probability and the one-hop cache coverage ratio, respectively. Legend "S-6000" and "T-6000" denote the result for simulation and theoretical analysis with a total vehicle number of 6000 respectively, similar for others.

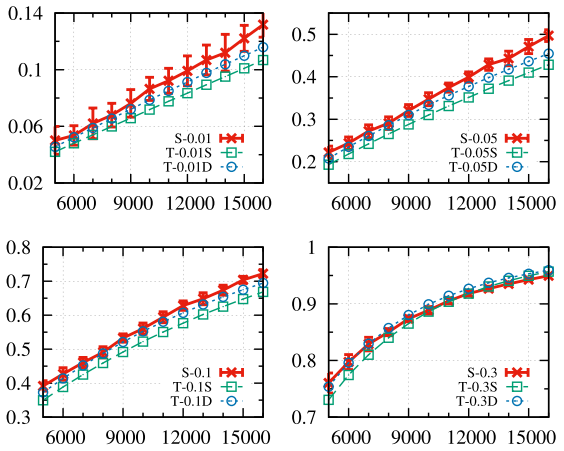

Figure 6. Comparison between simulations and theoretical analysis with the transmission radius set to 150 m. The *x*-axis and *y*-axis represent the total vehicle number and the one-hop cache coverage ratio, respectively, and the error bars represent the standard derivation in simulation. Legend "S-0.1" denotes the simulation result with the caching probability of 0.1, while "T-0.1S" and "T-0.1D" denote the theoretical result using the same and different rate parameters, respectively, similar for others.

ulations, which verifies that our analysis is in compliance with the simulated reality.

To clearly show the relationship between the cache coverage ratio and the vehicle density, we make plots alternatively in Figure 6, which also introduces another comparison between using different rate parameters in the intersection and non-intersection zones (legend ended by "D") and the same rate parameter for overall zones (legend ended by "S"). The *x*-axis represents the total vehicle number, and the *y*-axis represents the cache coverage ratio. As shown, there is only a slight difference between simulation and theoretical analysis when the caching probability is small. Besides, results of theoretical analysis using different rate parameters always get closer to simulated reality compared with using a single one for all zones, which proves the distinction for intersection zones is helpful.

The results with other transmission radius are similar, so we omit the plots.

We also verify the two-hop and three-hop cache coverage ratios. Because accurate computation is complex, Figure 7 shows the theoretical upper bounds and results from the approximate method instead. As shown, the upper bounds are closer to the simulation results with a larger total vehicle number, because there is higher probability that vehicles exist to forward the transmission so that the *n*-hop transmission range with the transmission radius of *R* is more approximate to the one-hop range with the radius of *nR*. Besides, results from the approximate method match well with simulation, and errors increase with high vehicle density because the approximate method uses the same rate parameters for all zones, but intersections become more important for connectivity in dense scenarios.

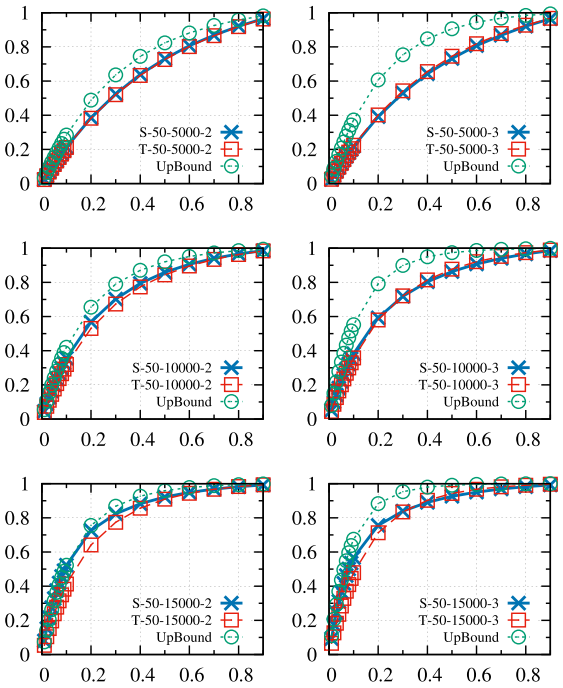

Figure 7. Results for two-hop cache coverage ratios. The *x*-axis and *y*-axis represent the caching probability and the cache coverage ratio, respectively. Legend "S-50-5000-2" and "T-50-5000-2" denote the simulation result and approximate computation result for two-hop with the transmission radius of 50 m and a total vehicle number of 5000, respectively, while "UpBound" denotes the theoretical upper bound, similar for others.

(c) *Different number of lanes:* We carry out simulations with different number of lanes in each direction to check whether the lane number affects the cache coverage ratio or not. As shown in Figure 8, we change the lane number from one to six in each direction in scenarios with different vehicle densities, but the cache coverage ratio scarcely changes when the vehicle density and caching rate remain the same. Thus, the validity of our analysis is also not affected by the lane number.

(d) *Different car-following models:* We also carry out simulations with different car-following models that characterize the microscopic behavior of vehicles. SUMO provides several car-following model implementations [10], and we choose five of them for comparison, that is, SUMOKrauβ (which is the default car-following model used in SUMO), SKOrig, SmartSK [11], Wiedemann [12], and Daniel1.[†‡] We set three lanes in each direction and run the simulations with different vehicle densities. Figure 9 shows the results. As we can observe, there is nearly no difference in the results using the five selected car-following models.

(e) *Different street lengths:* To check whether the street length has effects on the validity of our analysis, we execute simulations with other street lengths, that is, 800 and 1200 m. We keep the entire area of the simulation scenario unchanged, which is still $12 \times 12\,\text{km}^2$. We change the total vehicle number accordingly to maintain suitable vehicle densities. The results are shown in Figure 10, which proves that the analysis results match well with simulation in the scenarios with different street lengths and vehicle densities. Besides, using different rate parameters in the intersection and non-intersection zones can obtain much better results compared with using a single one for all zones in scenarios with larger street lengths. Note that the ranges of intersection zones also become larger, for example, 100 m in 1200-m-long street.

4.2. Validation of analysis on mobility impacts

We also conduct intensive simulations to verify the analysis that considers the mobility impacts on the cache coverage ratio presented in Section 3.2.

[†]A model proposed by Daniel Krajzewicz, lacking documentation.

[‡]The reason why we choose these five car-following models is that other models implemented in SUMO suffer from some problems such as Intelligent-Driver Model (IDM) [13].

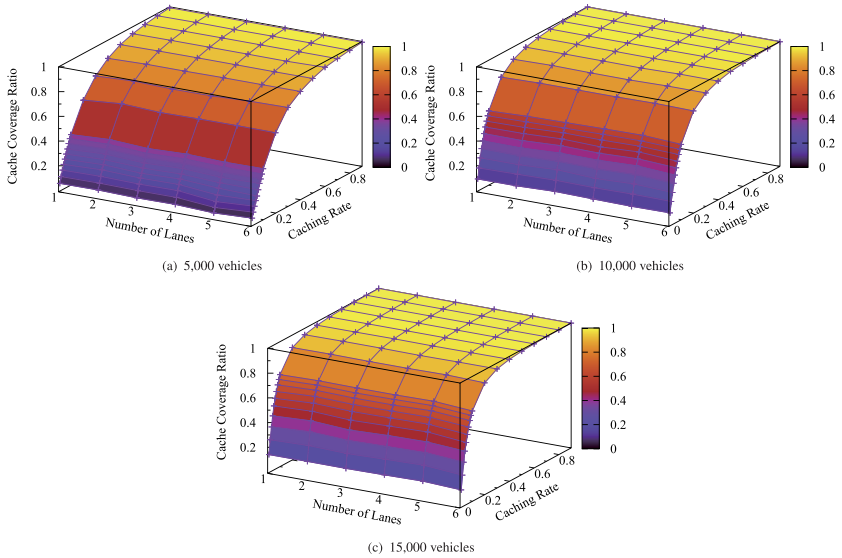

Figure 8. Results for different number of lanes in each direction.

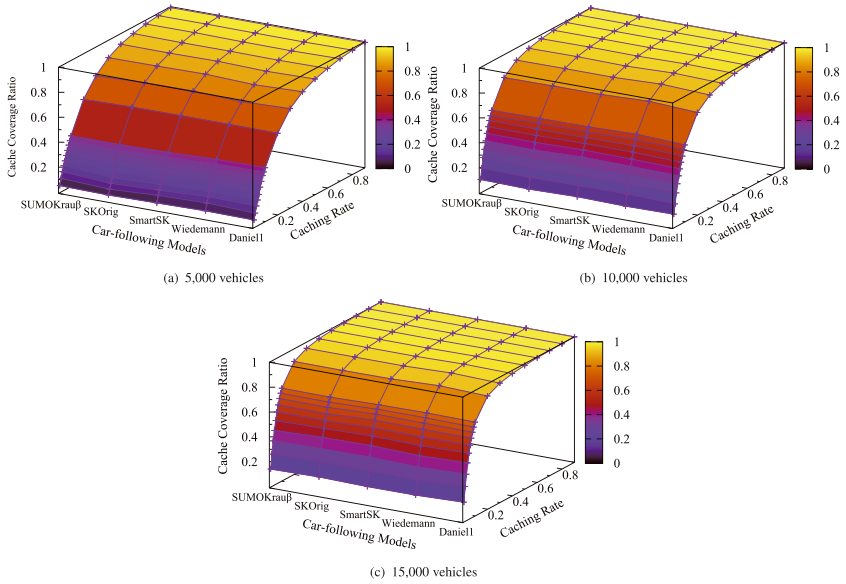

Figure 9. Results for different car-following models. The lane number is set to three in each direction.

4.2.1. Simulation scenario.

We use different scenarios that contain typical intersections with simple cyclic traffic lights just like those we use in the analysis. The signal phase length is 30 s, and the speed limit is 40 km/h. There are three lanes in each direction so that vehicles going to different directions do not affect each other. In the one-intersection scenario, vehicle flows are generated in all the four directions. For each flow, we turn on the "randomized-flows" flag in SUMO so that vehicles enter the scenario at random instants with a predefined mean headway, which approximately simulates an exponentially distributed vehicle headway. The fixed turning probabilities of vehicles at the intersection are set to the default values of SUMO, that is, vehicles go straight with a probability of 0.5, turn right with a probability of 0.3, and turn left with a probability of 0.2. In the two-intersection scenario, the second intersection is exactly at the north of the first one connected by a road, and vehicle flows are also generated in each direction. In both scenarios, we check snapshots at different instants after vehicle flows pass through the intersections to obtain the cache coverage ratio on the outgoing road. Each result shown in the succeeding text is an average of 100 independent runs.

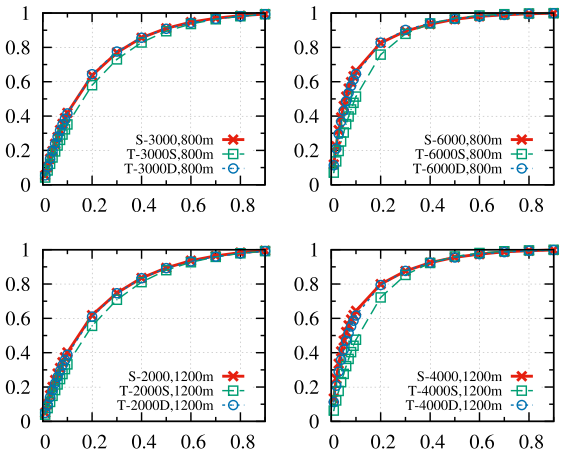

Figure 10. Results for different street lengths. The *x*-axis and *y*-axis represent the caching probability and the one-hop cache coverage ratio, respectively. Legend "S-3000,800m" denotes the simulation result with 3000 vehicles and the street length of 800 m, while "T-3000S,800m" and "T-3000D,800m" denote the theoretical result using the same and different rate parameters respectively, similar for others.

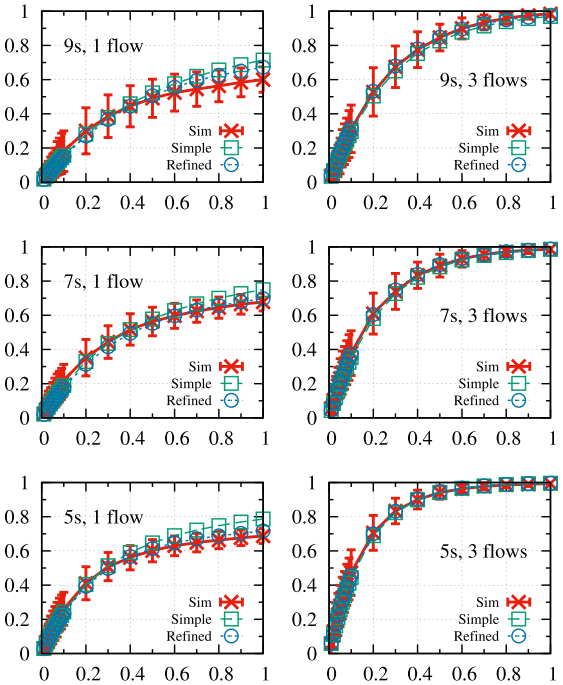

Figure 11. Comparison between simulations and theoretical analysis with the transmission radius set to 150 m. The *x*-axis and *y*-axis represent the caching probability and the one-hop cache coverage ratio, respectively, and the error bars represent the standard derivation in simulation. Mean arrival time of vehicles and the number of flows that contain cached vehicles are labeled in plots, for example, "9s, 3 flows". Legend "Sim," "Simple," and "Refined" denote the simulation result, results from simple, and refined computation methods, respectively, similar for others.

4.2.2. Validation results.

We present the validation results for both scenarios as follows.

(a) *One-intersection-away road:* In the one-intersection scenario, we use two different caching settings. The first one is that only the south road locates in the caching area, which means only vehicles coming from south have a certain caching rate. The second one is that vehicles from the east, south, and west all have a certain caching rate. Figure 11 shows the results for both settings.

As observed, results of the theoretical analysis again match well with simulation in both caching settings under scenarios with different mean entrance intervals of each vehicle flow. Comparatively, refined method gives a bit more accurate results. Better results are obtained in the second caching settings because of the more uniformly distributed caching vehicles.

We abbreviate the results for two-hop cache coverage ratio (or more) because they are quite similar with only a little higher difference between simulation and analysis.

(b) *Two-intersection-away road:* In the two-intersection scenario, we also use the same two caching settings as mentioned previously. Figure 12 shows the results, and we omit the results from the refined method that cannot generate much better results than the simple one.

As shown, the standard derivations of simulation results become much larger, which means that the increase of uncertainty on two-intersection-away roads and the analysis results are close to the average simulation results.

5. RELATED WORK

To improve the VANET performance, researchers have proposed many data dissemination mechanisms. Geo-based routing utilizes the location information to assist packet routing and forwarding. For instance, GyTAR [14] finds out the intersections that packets should pass through the shortest path, and then packets are greedily forwarded to the next intersection. Multiple factors are considered in forwarder selection to deal with the dynamic scenarios, including neighbor distance and channel frame error rate [15]. Carry-and-forward mechanism is introduced for disconnected scenarios, for example, UV-CAST [16] prefers boundary vehicles of connected network components as forwarders. However, these mechanisms cannot ensure good communication performance between distant vehicles, especially for scenarios of intermittent connectivity.

Some empirical caching mechanisms have been proposed for VANETs. In Hamlet [3], vehicles make caching decisions based on individual observations of data present around. Roadcast [4] considers content popularity for

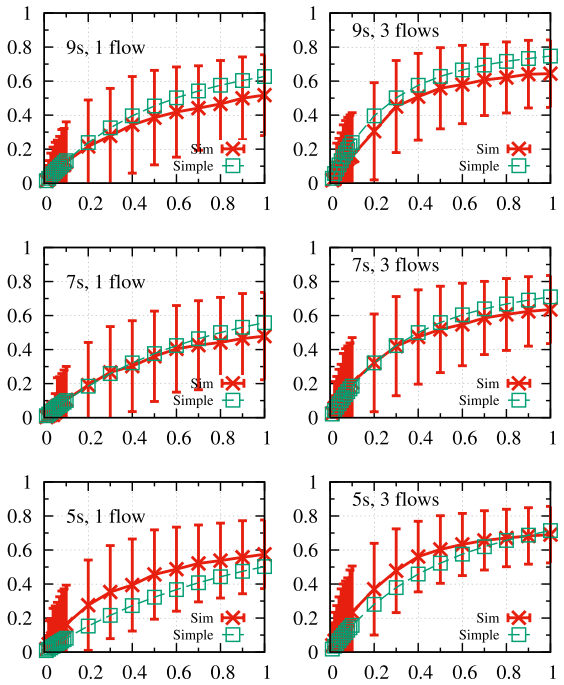

Figure 12. Comparison between simulations and theoretical analysis with the transmission radius set to 150 m. The *x*-axis and *y*-axis represent the caching probability and the one-hop cache coverage ratio, respectively, and the error bars represent the standard derivation in simulation. Mean arrival time of vehicles and the number of flows that contain cached vehicles are labeled in plots, for example, "9s, 3 flows". Legend "Sim" and "Simple" denote the result from simulation and simple computation method, respectively, similar for others.

specific applications in cache replacement when the cache buffer is full. Live VANET CDN [17] spreads cached copies around the requester position to amplify the caching effects.

Theoretical analysis for VANETs mainly concentrates on the network connectivity. Existing work [18] introduces percolation theory to study the critical parameters for connectivity, which include vehicle density and transmission radius. Another study utilizes the coverage process to analyze the same problem [19]. There is also work studying the obstacle effects on connectivity [20]. As for caching, only the one-hop mobility influence is discussed [21], which cares about local effects. Besides, researches on vehicle mobility model [22] try to characterize the patterns of vehicle mobility, which mainly aim to help simulation.

To summarize, existing work mainly presents specific data dissemination and caching mechanisms, or conducts theoretical analysis on VANET connectivity, while the analysis for caching effects on the network is missing to the best of our knowledge. Therefore, our work fills this blank as an initial step. Our analysis not only applies to caching but also applies for any scenario in which data can be accessed all around. A typical example is using buses as the Internet gateways or information dissemination source. Combining with the bus mobility model and distribution, our analysis can be utilized to assess the performance, and then guide the related strategy design. Besides, our analysis can also potentially be applied in the scenarios of crowdsourcing [23] and cellular networks [24,25].

6. CONCLUSION

We present the theoretical analysis for caching effects in urban VANETs. The cache coverage ratio is proposed to measure the caching effects in the network, and we find the quantitative relationship among the cache coverage ratio, vehicle density, transmission radius, caching rate, and so on. We also analyze the vehicle mobility impacts to predict the cache coverage ratio on surrounding roads of the caching area. Our analysis results match very well with simulation. Given the vehicle density and transmission range, our analysis model can be used to find the suitable caching rate for desired cache coverage, which is helpful for the design of caching mechanisms. Besides, the analysis method can be easily extended to other scenarios with multiple data access points, for example, using buses as gateways to access the Internet, deploying roadside units to serve as data sources. Our future work includes the extension of the analysis for other scenarios such as using buses as the data dissemination sources and the design of caching mechanisms.

ACKNOWLEDGEMENTS

This work is supported by NSFC (61272340, 61201245), and 973 Program (2014CB340405).

APPENDIX A: PROOF OF THEOREM 1

Because of the fact that the computation method of Q_1^{RS} for different road segments are similar, we only choose a typical one, that is, RS3, to show the concrete deduction process.

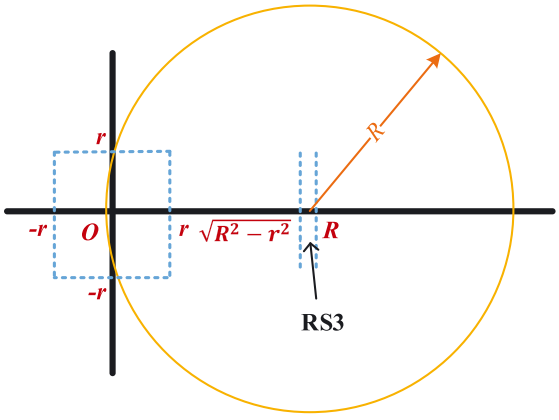

Figure A.1. The transmission range of a node on RS3.

As shown in Figure A.1, a node located at x on RS3 satisfies $x \in \left(\sqrt{R^2-r^2}, R\right]$, so the transmission range can be divided into three parts, that is, $(r, x+R]$ located in the non-intersection zone, $(x-R, r]$ located in the intersection zone, and $\left[-\sqrt{R^2-x^2}, \sqrt{R^2-x^2}\right]$ located in the intersection zone on the vertical road. Thus, we can compute $Q_1^{RS3}(x)$ as follows.

$$\begin{aligned}
Q_1^{RS3}(x) &= 1 - P(\text{no caching node exists in } (x-R, r] \text{ or} \\
&\qquad (r, x+R]) \text{ or } \left[-\sqrt{R^2-x^2}, \sqrt{R^2-x^2}\right]) \\
&= 1 - \sum_{n=0}^{\infty} e^{-\lambda_1(r+R-x)} \frac{[\lambda_1(r+R-x)]^n}{n!}(1-\mu)^n \cdot \\
&\quad \sum_{n=0}^{\infty} e^{-\lambda_2(x+R-r)} \frac{[\lambda_2(x+R-r)]^n}{n!}(1-\mu)^n \cdot \\
&\quad \sum_{n=0}^{\infty} e^{-\lambda_1 \cdot 2\sqrt{R^2-x^2}} \frac{(\lambda_1 \cdot 2\sqrt{R^2-x^2})^n}{n!}(1-\mu)^n \\
&= 1 - e^{\left[-\lambda_1(r+R-x)-\lambda_2(x+R-r)-\lambda_1 \cdot 2\sqrt{R^2-x^2}\right]\cdot\mu}.
\end{aligned}$$

APPENDIX B: PROOF OF THEOREM 2

Let the reference node locate at the origin, and there are other nodes on the axis with the node interval following an exponential distribution. The one-hop distance of a node is determined by the farthest node within the transmission range. Because of symmetry, we only need to consider one direction. Thus, the expected one-hop distance of the reference node is equal to the coordinate of the farthest node located in $[0, R]$. So we first compute the probability that the farthest node locates at $x (0 \le x \le R)$.

Let $P_n(x)$ denote the probability that the nth node in $[0, R]$ except the reference node, which is at the origin, locates at x. We have the following formulas.

$$\begin{aligned}
P_1(x) &= \lambda e^{-\lambda x}, \\
P_2(x) &= \int_0^x \lambda e^{-\lambda x_1} \cdot \lambda e^{-\lambda(x-x_1)} \mathrm{d}x_1 \\
&= e^{-\lambda x}\lambda^2 x, \\
P_3(x) &= \int_0^x \lambda e^{-\lambda x_1} \int_0^{x-x_1} \lambda e^{-\lambda x_2} \cdot \lambda e^{-\lambda(x-x_1-x_2)} \mathrm{d}x_2 \mathrm{d}x_1 \\
&= \frac{1}{2} e^{-\lambda x}\lambda^3 x^2, \\
&\cdots, \\
P_n(x) &= \int_0^x \lambda e^{-\lambda x_1} \int_0^{x-x_1} \lambda e^{-\lambda x_2} \int_0^{x-x_1-x_2} \lambda e^{-\lambda x_3} \cdots \\
&\qquad \int_0^{x-x_1-x_2-\cdots-x_{n-1}} \lambda e^{-\lambda x_n} \cdot \\
&\qquad \lambda e^{-\lambda(x-x_1-x_2-\cdots-x_n)} \mathrm{d}x_n \mathrm{d}x_{n-1} \cdots \mathrm{d}x_1 \\
&= \frac{e^{-\lambda x}\lambda^n x^{n-1}}{(n-1)!}.
\end{aligned}$$

Let $Q_n(x)$ denote the probability that there are n nodes in $[0, R]$ except the reference node and the nth node locates at x. We have the following formula.

$$\begin{aligned}
Q_n(x) &= P_n(x) \int_{R-x}^{\infty} \lambda e^{-\lambda t} \mathrm{d}t \\
&= \frac{e^{-\lambda R}\lambda^n x^{n-1}}{(n-1)!}.
\end{aligned}$$

Therefore, the expected one-hop distance can be computed as follows.

$$\begin{aligned}
E(D) &= \sum_{n=0}^{\infty} \int_0^R Q_n(x) x \mathrm{d}x \\
&= R - \frac{1 - e^{-\lambda R}}{\lambda}.
\end{aligned}$$

REFERENCES

1. Wu C, Ohzahata S, Kato T. Fuzzy logic based multihop broadcast for high-density vehicular ad hoc networks. In *2010 IEEE Vehicular Networking Conference (VNC)*. IEEE, New Jersey, USA, 2010; 17–24.
2. Wu C, Ohzahata S, Kato T. A broadcast path diversity mechanism for delay sensitive vanet safety applications. In *2011 IEEE Vehicular Networking Conference (VNC)*. IEEE, Amsterdam, Netherlands, 2011; 171–176.
3. Fiore M, Mininni F, Casetti C, Chiasserini C-F. To cache or not to cache? In *IEEE INFOCOM 2009*. IEEE, Rio de Janeiro, Brazil, 2009; 235–243.
4. Zhang Y, Zhao J, Cao G. Roadcast: a popularity aware content sharing scheme in vanets. *ACM SIGMOBILE Mobile Computing and Communications Review* 2010; **13**(4): 1–14.
5. Jacobson V, Smetters DK, Thornton JD, Plass MF, Briggs NH, Braynard RL. Networking named content. In *Proceedings of the 5th International Conference on Emerging Networking Experiments and Technologies*. ACM, Rome, Italy, 2009; 1–12.
6. Li Y, Lin T, Tang H, Sun P. A chunk caching location and searching scheme in content centric networking. In *2012 IEEE International Conference on Communications (ICC)*. IEEE, Ottawa, Canada, 2012; 2655–2659.
7. Krajzewicz D, Erdmann J, Behrisch M, Bieker L. Recent development and applications of SUMO - Simulation of Urban MObility. *International Journal On Advances in Systems and Measurements* 2012; **5**(3&4): 128–138.
8. Roess RP, Prassas ES, McShane WR. *Traffic Engineering*. Pearson/Prentice Hall: Upper Saddle River, New Jersey, 2004.

9. Greenberg I. The log normal distribution of headways. *Australian Road Research* 1966; **2**(7): 8–14.
10. Definition of vehicles, vehicle types and routes in sumo. Available from: http://sumo.dlr.de/wiki/Definition_of_Vehicles,_Vehicle_Types,_and_Routes [Accessed on 16th October 2015].
11. Krauß S. Microscopic modeling of traffic flow: investigation of collision free vehicle dynamics. *Ph.D. Thesis*, Universitat zu Koln, Koeln, Germany, 1998.
12. Wiedemann R. Simulation des straßenverkehrsflußes. *Technical Report Heft 8 der Schriftenreihe des IfV, 1974*, Institut für Verkehrswesen, Universität Karlsruhe, Karlsruhe, Germany, 1974.
13. Treiber M, Helbing D. Realistische mikrosimulation von strassenverkehr mit einem einfachen modell. In *16th Symposium Simulationstechnik ASIM,* vol. 2002, Rostock, Germany, 2002; 80.
14. Jerbi M, Meraihi R, Senouci SM, Ghamri-Doudane Y. Gytar: improved greedy traffic aware routing protocol for vehicular ad hoc networks in city environments. In *Proceedings of the 3rd International Workshop on Vehicular Ad Hoc Networks*. ACM, Los Angeles, California, USA, 2006; 88–89.
15. Katsaros K, Dianati M, Tafazolli R, Kernchen R. Clwpr: A novel cross-layer optimized position based routing protocol for vanets. In *2011 IEEE Vehicular Networking Conference (VNC)*. IEEE, Amsterdam, Netherlands, 2011; 139–146.
16. Viriyasitavat W, Bai F, Tonguz OK. Uv-cast: An urban vehicular broadcast protocol. In *2010 IEEE Vehicular Networking Conference (VNC)*. IEEE, New Jersey, USA, 2010; 25–32.
17. Nakamura N, Niimi Y, Ishihara S. Live vanet cdn: Adaptive data dissemination scheme for location-dependent data in vanets. In *2013 IEEE Vehicular Networking Conference (VNC)*. IEEE, Boston, 2013; 95–102.
18. Jin X, Su W, Wei Y. Quantitative analysis of the vanet connectivity: theory and application. In *2011 IEEE 73rd Vehicular Technology Conference (VTC Spring)*. IEEE, Budapest, Hungary, 2011; 1–5.
19. Shioda S. Connectivity of vehicular ad hoc networks in downtown scenarios. In *Ad Hoc Networks, Lecture Notes of the Institute for Computer Sciences, Social Informatics and Telecommunications Engineering*. Vol. 89, Springer Berlin Heidelberg, 2012; 177–192.
20. Almiron MG, Goussevskaia O, Loureiro AA, Rolim J. Connectivity in obstructed wireless networks: from geometry to percolation. In *Proceedings of the Fourteenth ACM International Symposium on Mobile Ad Hoc Networking and Computing*. ACM, Bangalore, India, 2013; 157–166.
21. Attia O, ElBatt T. On the role of vehicular mobility in cooperative content caching. In *2012 IEEE Wireless Communications and Networking Conference Workshops (WCNCW)*. IEEE, Paris, France, 2012; 350–354.
22. Harri J, Filali F, Bonnet C. Mobility models for vehicular ad hoc networks: a survey and taxonomy. *IEEE Communications Surveys & Tutorials* 2009; **11**(4): 19–41.
23. Zhang H, Xu Z, Du X. Context-aware participant recruitment mechanism in mobile crowdsourcing. *Wireless Communications and Mobile Computing,* accepted 2015.
24. Xiao Y, Leung KK, Pan Y, Du X. Architecture, mobility management, and quality of service for integrated 3g and wlan networks. *Wireless Communications and Mobile Computing* 2005; **5**(7): 805–823.
25. Lin Z, Du L, Gao Z, Huang L, Du X. Efficient device-to-device discovery and access procedure for 5g cellular network. *Wireless Communications and Mobile Computing,* accepted 2015, DOI: 10.1002/wcm.2602.

AUTHORS' BIOGRAPHIES

Chaoyi Bian received his BS degree from Peking University, China in 2009. He is currently a PhD candidate in the School of Electronics Engineering and Computer Science at Peking University. His research interests are in the areas of wireless ad hoc networks, vehicular ad hoc networks, and named data networking.

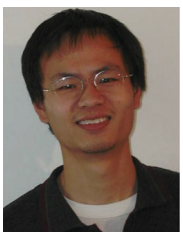

Tong Zhao received his MS degree in 2002, and his PhD degree in 2014, all in the School of Electronics Engineering and Computer Science from Peking University, China. He is currently an engineer at Peking University. His major research interest is wireless networks and mobile computing.

Xiaoming Li received his PhD in computer science from Stevens Institute of Technology (USA) in 1986 and now is a Professor at Peking University. His research interests include Web search and mining, online social network analysis. He is an editor of Concurrency and Computation, and an editor of Networking Science.

Xiaojiang Du is an associate professor at Temple University. He received his BE degree from Tsinghua University, China, in 1996 and his PhD degree from the University of Maryland, College Park in 2003, all in Electrical Engineering. His research interests are security, systems, wireless networks, and computer networks. He has published over 160 journal and conference papers in these areas. He is a life Member of ACM.

Wei Yan received her MS degree in computer science from National University of Defence Technology in 1990. She is currently an associate professor in Peking University. Her major research interests include mobile networks, vehicular networks, and mobile computing.